Food Bioprocess Technol (2016) 9:101–112
DOI 10.1007/s11947-015-1602-0

ORIGINAL PAPER

Physico-Mechanical Characterization and Antimicrobial Properties of Fish Protein Isolate/Fish Skin Gelatin-Zinc Oxide (ZnO) Nanocomposite Films

Yasir Ali Arfat[1] · **Soottawat Benjakul**[1] · **Thummanoon Prodpran**[2] · **Punnanee Sumpavapol**[1] · **Ponusa Songtipya**[2]

Received: 2 December 2014 / Accepted: 21 September 2015 / Published online: 30 September 2015

Abstract Antimicrobial nanocomposite films based on fish protein isolate (FPI)/fish skin gelatin (FSG) (1/1 *w*/*w*) prepared at pH 3 and 11 containing zinc oxide nanoparticles (ZnONP) at different levels (0–4 % *w*/*w* of protein) were characterised. At both pH 3 and pH 11, tensile strength (TS) increased, whilst elongation at break (EAB) and water vapour permeability (WVP) decreased as ZnONP content increased ($p<0.05$). FPI/FSG-ZnO nanocomposite films had lower transparency, b^*-values (yellowness), and ΔE^*-values (total colour difference) than the control FPI/FSG film ($p<0.05$). Attenuated total reflectance-Fourier transform infrared (ATR-FTIR) spectroscopic analysis revealed that there was interaction between ZnONP and protein in the film matrix. Based on thermogravimetric analysis, ZnONP could improve the thermal stability of the nanocomposite films. X-ray diffraction (XRD) analysis confirmed the crystalline structure of the ZnONP in the nanocomposite films. FPI/FSG-ZnO nanocomposite films, especially those prepared at pH 3, exhibited strong antibacterial activity and thus could be used as an active food packaging material.

Keywords Biopolymer film · Fish protein isolate · Fish skin gelatin · ZnO nanoparticles · Nanocomposite material · Antimicrobial packaging

✉ Yasir Ali Arfat
yasir.arfat123@gmail.com

[1] Department of Food Technology, Faculty of Agro-Industry, Prince of Songkla University, Hat Yai, Songkhla 90112, Thailand

[2] Department of Material Product Technology, Faculty of Agro-Industry, Prince of Songkla University, Hat Yai, Songkhla 90112, Thailand

Introduction

Biopolymers produced from various natural resources such as proteins, starch and cellulose have been considered as attractive alternatives for non-biodegradable petroleum-based plastics since they are abundant, renewable, inexpensive, environmentally friendly and biodegradable. Biopolymers not only act as barriers to moisture, water vapour, gases and solutes, but also serve as carriers of a wide variety of additives, such as antimicrobials, antioxidants, antifungal agents, colorants and other nutrients (Han 2000). Amongst biopolymer materials, proteins from different sources have been impressively used for the development of biodegradable films due to their abundance, diverse molecularity and good film-forming ability (Iwata et al. 2000; Prodpran et al. 2007).

Fish protein isolate (FPI) prepared by alkaline solubilisation was reported as the promising starting material for preparation of films with negligible yellow discolouration (Tongnuanchan et al. 2011). However, FPI based film is rigid and shows poor water vapour barrier property, owing to the hydrophilicity of amino acids in protein molecules and to the significant amounts of hydrophilic plasticizers required for film flexibility (Prodpran et al. 2007; McHugh et al. 1994). Recently, properties of FPI films from yellow stripe trevally, an abundant trash dark muscle fish, could be modified by blending with fish skin gelatin (FSG) at a ratio of 1:1 with lower glycerol content (30 %) at both acidic and alkaline pH. The blend between FPI and FSG was compatible, and the interaction between these two different proteins via hydrogen bond and other interactions was enhanced. Blend films showed the improved mechanical and water vapour barrier properties, compared with FPI films (Arfat et al. 2014). However, FPI/FSG blend films still have poorer mechanical as well as water vapour barrier property, in comparison with synthetic films.

Nanotechnology has been implemented to biopolymer films for improving mechanical, thermal and water vapour barrier properties (Kovacevic et al. 2008). Furthermore, it can generate active packaging systems (Espitia et al. 2013). Bionanocomposites represent the new generation of nanocomposites and comprise of natural polymer matrix and organic/inorganic filler with at least one dimension on the nanometre scale (Alebooyeh et al. 2012). Nanofillers have excellent interfacial interactions on polymer branches due to their large specific surface area and high surface energy thus significantly enhancing polymer properties such as thermal, mechanical and water barrier properties (Kovacevic et al. 2008). Recently, the incorporation of ZnONP as functional filler into the biopolymer films such as starch-based films have been reported to improve mechanical and water vapour barrier properties (Alebooyeh et al. 2012; Yu et al. 2009). ZnO is currently listed as a generally recognised as safe (GRAS) material by the Food and Drug Administration (21CFR182.8991) and has previously shown strong antimicrobial activity against food borne pathogens and spoilage bacteria (Espitia et al. 2013). However, there is no report on ZnO nanocomposite protein films, especially those from FPI and FSG. This work aimed to characterise FPI/FSG-ZnO nanocomposite films and to determine antimicrobial activity against Gram-positive *Listeria monocytogenes* (food borne pathogen) and Gram-negative *Pseudomonas aeruginosa* (food spoilage bacteria).

Materials and Methods

Materials

Zinc oxide nanoparticles (ZnONP) (particle size 20–40 nm, specific surface area 26.22 m^2/g) were purchased from NanoMaterials Technology Co., Ltd. (Bangkok, Thailand). Sodium chloride (NaCl), glycerol, sodium hydroxide (NaOH) and hydrochloric acid (HCl) were obtained from Merck (Darmstadt, Germany). Commercial FSG from tilapia (*Oreochromis niloticus*) (~240 bloom) was purchased from Lapi Gelatine S.p.A (Empoli, Italy) and contained 87.5 % protein (wet weight basis) as determined by the Kjeldahl method using the conversion factor of 5.4 (Jongjareonrak et al. 2010). FSG contained 11.2 % moisture, 0.5 % lipid and 0.4 % ash content (wet weight basis). All chemicals were of analytical grade. *Listeria monocytogenes* DMST 1327 was obtained from the Department of Medical Sciences, Ministry of Public Health, Nonthaburi, Thailand, and *Pseudomonas aeruginosa* TISTR 781 was obtained from the Thailand Institute of Scientific and Technological Research (TISTR), Thailand.

Preparation of Fish Samples

Fresh yellow stripe trevally (*Selaroides leptolepis*) with an average weight of 90–100 g/fish was purchased from a local market in Hat Yai, Songkhla Province, Thailand. Fish were kept in ice with a fish/ice ratio of 1:2 (*w*/*w*) and transported to the Department of Food Technology, Prince of Songkla University within 30 min. Upon the arrival, fish were immediately washed, filleted and minced to uniformity using a mincer with a hole diameter of 0.5 cm.

Preparation of Fish Protein Isolate

Prior to the isolation of fish protein, the prepared mince was subjected to washing as per the method of Tongnuanchan et al. (2011) with slight modifications. Fish mince was homogenised with 5 volumes of cold 0.05 M NaCl (2−4 °C) at a speed of 13,000 rpm for 2 min, using an IKA Labortechnik homogeniser (Selangor, Malaysia). The washed mince was filtered through two layers of cheese-cloth. The washing process was repeated twice. Washed mince obtained was stored in ice until used.

Washed mince was added with cold distilled water at the ratio of 1:9 (*w*/*v*), followed by homogenisation for 1 min at a speed of 13,000 rpm. The pH of the homogenates was then adjusted to 11 using 2 M NaOH. The resulting mixture was centrifuged at 10,000×*g* for 20 min at 4 °C using a refrigerated centrifuge (Avanti-JE Centrifuge, Beckman 163 Coulter Inc., Fullerton, CA, USA). The supernatant was collected, and the pH was adjusted to 5.5 using 2 M HCl. The precipitate was then filtered through four layers of cheese-cloth. The retentate was dewatered by centrifugation at 12,000×*g* for 20 min at 4 °C. The final pH of the sample was adjusted to pH 7.0 using 2 M NaOH. The sample was referred to as "fish protein isolate; FPI". FPI was used for film preparation. Fish protein isolate contained 14.02 % protein (as determined by the Kjeldahl method using the conversion factor of 6.25), 84.53 % moisture, 0.66 % lipid and 0.34 % ash content (wet weight basis).

Preparation of FPI/FSG-ZnONP FFS and Film Casting

The film-forming solution from FPI (FPI–FFS) was prepared according to the method of Chinabhark et al. (2007). FPI was added with 3 volumes of distilled water and homogenised at 13,000 rpm for 1 min using a homogeniser. Subsequently, the pH of the mixture was adjusted to 3 or 11 using 1 N HCl and 1 N NaOH, respectively, to solubilise the protein. The solutions were filtered through two layers of cheese-cloth to remove undissolved debris. The protein concentration of the filtrate determined by the Kjeldahl method using the conversion factor of 6.25 (AOAC 2000) was adjusted to 3 % (*w*/*v*). Glycerol at 30 % (*w*/*w*) of protein was used as a plasticiser.

The mixture was stirred gently for 30 min at room temperature and was used for preparing blend FFS.

FFS from FSG (FSG–FFS) was prepared by adding Tilapia gelatin powder in distilled water to obtain the protein concentration of 3 % (*w*/*v*). The pH of the mixture was adjusted to 3 or 11 using 1 N HCl and 1 N NaOH, respectively. The mixture was heated at 70 °C for 30 min. Glycerol at concentrations of 30 % (*w*/*w*) of protein content was used as a plasticiser. For each pH, film-forming solution of the FPI/FSG blend was prepared by mixing FPI–FFS and FSG–FFS at a ratio of 1:1 (*v*/*v*).

ZnONP (0, 1, 2, 3 and 4 % of protein, *w*/*w*) were mixed with distilled water, and the suspension was stirred for 5 min and then homogenised for 1 min at the speed of 5000 rpm (IKA Labortechnik homogeniser, Selangor, Malaysia). ZnONP suspension was gradually added into FPI/FSG blend film-forming solution in droplets. The mixture was stirred for 5 min. Final volume was made up to 100 ml using distilled water previously adjusted to the corresponding pH. To improve the mixing and uniform distribution of protein and ZnONP, the suspensions were homogenised with three passes through a high pressure homogeniser (Microfluidizer M-110EH, Microfluidics Corp., Newton, MA, USA) with an operating pressure of 1500 bars. Suspensions were gently stirred for 30 min at room temperature and were referred to as a film-forming suspension (FFSp). Prior to casting, FFSp samples were degassed for 10 min using the sonicating bath (Elmasonic S 30H, Singen, Germany). To prepare the film, 4 g of FFSp was cast onto a rimmed silicone resin plate (5×5 cm^2), air-blown for 12 h at 25 °C, followed by drying in an environmental chamber (Binder GmbH, Tuttlingen, Germany) at 25±0.5 °C and 50±5 % relative humidity (RH) for 24 h. Dried film samples were manually peeled off and subjected to analyses.

Determination of Physicochemical Properties of FPI/FSG-ZnONP Nanocomposite Films

Prior to testing, films were conditioned for 48 h at 50±5 % RH at 25±0.5 °C. For XRD, attenuated total reflectance-Fourier transform infrared (ATR-FTIR), thermo-gravimetric analysis (TGA) and scanning electron microscopy (SEM) analyses, films were dried in a desiccator containing dried silica gel for 1 week and in a desiccator containing phosphorus pentoxide (P_2O_5) for 2 weeks at room temperature (28−30 °C) to obtain the most dehydrated films and to minimise the plasticising effect due to water.

Film Thickness

The thickness of film was measured using a digital micrometer (Mitutoyo, Model ID-C112PM, Serial No. 00320, Mitutoyo Corp., Kawasaki-shi, Japan). Ten random locations around each film sample were used for thickness determination.

Mechanical Properties

Tensile strength (TS) and elongation at break (EAB) of films were determined as described by Iwata et al. (2000) using the universal testing machine (Lloyd Instruments, Hampshire, UK). Ten samples (2 cm×5 cm) with initial grip length of 3 cm were used for testing. The samples were clamped and deformed under tensile loading using a 100 N load cell with the cross-head speed of 30 mm/min until the samples were broken. The maximum load and the final extension at break were used for calculation of TS and EAB, respectively.

Water Vapour Permeability

Water vapour permeability (WVP) was measured using a modified ASTM method as described by Shiku et al. (2004). The film was sealed on an aluminium permeation cup containing dried silica gel (0 % RH) with silicone vacuum grease and a rubber gasket to hold the film in place. The cups were placed in a desiccator containing the distilled water at 30 °C. The cups were weighed at 1 h intervals over a 10-h period. WVP of the film was calculated as follows:

$$\mathrm{WVP}\left(\mathrm{gm}^{-1}s^{-1}\mathrm{Pa}^{-1}\right) = wlA^{-1}t^{-1}(P_2{-}P_1)^{-1}$$

where w is the weight gain of the cup (g); l is the film thickness (m); A is the exposed area of film (m^2); t is the time of gain (s); (P_2–P_1) is the vapour pressure difference across the film (4244.9 Pa at 30 °C).

Colour Values

Colour values of film were determined using a CIE colourimeter (Hunter associates laboratory, Inc., Reston, VA, USA). Colour of the film was expressed as L^* (lightness), a^* (redness/greenness) and b^* (yellowness/blueness) values. Total difference in colour (ΔE^*) was calculated according to the following equation (Gennadios et al. 1996):

$$\Delta E^* = \sqrt{\left(\Delta L^*\right)^2 + \left(\Delta a^*\right)^2 + \left(\Delta b^*\right)^2}$$

where ΔL^*, Δa^* and Δb^* are the differences between the corresponding colour parameters of the samples and that of white standard (L^*=92.71, a^*=−0.92, b^*=0.46).

Light Transmittance and Transparency Values

The light transmittance of films was measured at the ultraviolet and visible range (200–800 nm) using a UV–visible

spectrophotometer (Shimadzu UV-1800, Kyoto, Japan) according to the method of Shiku et al. (2004). The transparency value of film was calculated using the following equation (Han and Floros 1997):

$$\text{Transparency value} = \frac{-\log T_{600}}{x}$$

where T_{600} is the fractional transmittance at 600 nm and x is the film thickness (mm). The greater transparency value represents the lower transparency of film.

Characterisation of the Selected Films

FPI/FSG films (pH 3 and pH 11) incorporated with 3 % ZnONP were subjected to characterisation in comparison with the control FPI/FSG films with corresponding pH.

Wide Angle X-ray Diffraction Measurement

Wide-angle X-ray diffraction (WAXD) measurements were carried out by using a wide-angle X-ray diffractometer (Philips X'Pert MPD, Almelo, Netherland) with the following conditions: Cu source (copper sources emit X-rays with a wavelength, λ=1.5406 Å); operating at room temperature; 40 kV and 30 mA current. The samples were cut into the circular shape of 30 mm diameter and placed in a sample holder. Then, the set was placed inside the chamber of the apparatus in order to perform the measurements. The measurement angles (2θ) were varied from 5° to 75°.

Attenuated Total Reflectance-Fourier Transform Infrared Spectroscopy Measurement

FTIR spectra of film samples were determined using a Bruker Model Equinox 55 FTIR spectrometer (Bruker Co., Ettlingen, Germany) equipped with a horizontal ATR Trough plate crystal cell (45° Zinc Selenide (ZnSe); 80 mm long, 10 mm wide and 4 mm thick) (PIKE Technology Inc., Madison, WI, USA) at 25 °C as described by Nuthong et al. (2009). Samples were placed onto the crystal cells, and the cells were clamped into the mount of the FTIR spectrometer. The spectra in the range of 650–4000 cm^{-1} with automatic signal gain were collected in 32 scans at a resolution of 4 cm^{-1} and were ratioed against a background spectrum recorded from the clean empty cell at 25 °C.

Thermo-Gravimetric Analysis

Dried films were scanned using a thermo-gravimetric analyser (TGA-7, Perkin Elmer, Norwalk, CT, USA) from 40 to 600 °C at a rate of 10 °C/min (Nuthong et al. 2009). Nitrogen was used as the purge gas at a flow rate of 20 ml/min. The thermal degradation temperature (T_d) and weight loss (Δw) during the heating cycle was estimated using the associated software (Nuthong et al. 2009).

Scanning Electron Microscopy Visualisation

Morphology of surface and freeze-fractured cross-section of film samples were visualized using a scanning electron microscope (SEM) (Quanta400, FEI, Eindhoven, the Netherlands) at an accelerating voltage of 15 kV. Prior to visualisation, the film samples were mounted on brass stub and sputtered with gold in order to make the sample conductive, and photographs were taken at ×7000 magnification for surface. For cross-section, freeze-fractured films were mounted around stubs using double-sided adhesive tape, coated with gold and observed at the ×4000 magnification.

Determination of Antimicrobial Activities of Films

Antimicrobial activity of film samples was assessed using the disk diffusion method according to the Clinical and Laboratory Standards Institute (2007, 2010) with some modification. The zone of inhibition on solid media was used for determining the antimicrobial activity of films against typical food pathogenic and spoilage bacteria including Gram-positive bacteria (*Listeria monocytogenes*) and Gram-negative bacteria (*Pseudomonas aeruginosa*). Bacteria stored at −80 °C were grown twice in Tryptic soy broth (Merck, Darmstadt, Germany) and incubated for 18 h at 35±2 °C. The bacterial suspension was adjusted to achieve the turbidity of McFarland standard solution 0.5 resulting in an inoculums containing approximately 10^6–10^7 CFU/ml. Film samples were cut into a disc shape with a 10-mm diameter using a circular knife and then placed on Mueller Hinton agar (Merck, Darmstadt, Germany), which had been previously smeared with 100 μl of inoculums of tested bacteria. The plates were then incubated at 35±2 °C for 18 h. The antimicrobial activity of nanocomposite films was determined by measuring the diameter of the inhibition zone around each film.

Statistical Analysis

Experiments were run in triplicate using three different lots of samples. Data were subjected to analysis of variance (ANOVA), and mean comparisons were carried out by Duncan's multiple range test (Steel and Torrie 1980). Statistical analysis was performed using the Statistical Package for Social Science (SPSS 17.0 for windows, SPSS Inc., Chicago, IL, USA). Statistical significance was set at $p<0.05$.

Results and Discussion

Physicochemical Properties of FPI/FSG-ZnO Nanocomposite Films

FPI/FSG films prepared at pH 3 and pH 11, containing ZnONP at varying levels, exhibited different properties.

Film Thickness

Thickness of FPI/FSG films prepared at pH 3 and pH 11 with various levels of ZnONP is shown in Table 1. Different pHs (3 or 11) had no pronounced impact on thickness of the resulting films ($p>0.05$). The extended or stretched chains of both FPI (myosin heavy chain) and FSG (both alpha 1 and alpha 2 chains) facilitated the molecular alignment to form the ordered network in the similar fashion, regardless of pH used. It was noted that the thickness of films increased as the levels of ZnONP incorporated increased ($p<0.05$), irrespective of pH of FFS. The increases in the thickness with the addition of ZnONP could be due to the increase in solid content associated with ZnONP. Nanoparticles distributed throughout the film matrix resulted in the increased thickness of resulting films after drying. This behaviour was also observed by Sothornvit et al. (2009) for whey protein isolate-based nanocomposite films.

Mechanical Properties

Mechanical properties of FPI/FSG films prepared at pH 3 and pH 11 without and with the addition of ZnONP at various levels are shown in Table 1. The control FPI/FSG film (without ZnONP) prepared at pH 11 had higher TS ($p<0.05$) but lower EAB ($p>0.05$) than those prepared at pH 3. Alkaline pH might favour the solubilisation of protein molecules, which resulted in greater extension or stretching of proteins. The subsequent alignment of partially denatured myofibrillar protein and the stretched fibrous gelatin molecules (both alpha 1 and alpha 2 chains) more likely led to the formation of strong film network with high junction zones. Moreover, it was reported that FPI prepared at acidic pH had higher degradation (Tongnuanchan et al. 2011). As a result, the lower strength of films containing FPI prepared at pH 3 was obtained. The slightly increased EAB of film prepared at acidic pH was more likely caused by the presence of weaker bonds stabilising film matrix (Tongnuanchan et al. 2011).

When ZnONP was incorporated into the film, ZnONP exhibited an obvious reinforcing effect. As the ZnONP content increased up to 3 %, TS increased, but the EAB of the composites decreased ($p<0.05$), irrespective of the pH of FFS. However, the films prepared at pH 11 had higher TS ($p<0.05$) and lower EAB ($p>0.05$) as compared with those prepared at pH 3. The higher TS of ZnONP added films prepared at pH 11 was likely due to the enhanced salt bridges formation between Zn^{2+} and negatively charged residues, mainly COO^{-} of protein side chains or C-termini. Similar interactions in ZnO–whey protein nanocomposite were reported (Shi et al. 2008). A significant increase ($p<0.05$) in TS with ZnONP incorporation was consistent with other studies on reinforced protein films by nanoparticles (Rouhi et al. 2013). The ZnONP incorporated into the protein matrix limited the moving scale of protein chain segments and generated an interactive force against the protein chains. This was evidenced by increased TS but decreased EAB. The nanoparticles have high surface energy and large specific surface area, giving rise to strong interfacial interactions between polymer and the nanoparticles and bring about a significant enhancement in the polymer properties (Kovacevic et al. 2008; Rouhi et al. 2013).

However, at the ZnONP concentration above 3 %, the sharp decreases in both TS and EAB were noticeable ($p<0.05$). The decrease of the mechanical strength of the nanocomposite film might be attributed to the non-uniform

Table 1 Film thickness, mechanical properties and water vapour permeability of FPI/FSG-ZnONP films

pH level	ZnONP level (% *w*/*w*)	Thickness (mm)	TS (MPa)	EAB (%)	WVP ($\times 10^{-11}$ g m^{-1} s^{-1} Pa^{-1})
	0	0.036±0.001d	13.07±0.60d	64.31±5.64ab	3.37±0.18bc
	1	0.038±0.001cd	14.29±0.63c	61.43±4.55bc	3.11±0.22cd
11	2	0.039±0.001bc	15.83±0.86b	56.82±4.48cd	2.67±0.18e
	3	0.041±0.001ab	17.76±0.93a	49.20±4.14ef	2.09±0.14f
	4	0.042±0.002a	9.43±0.53f	39.43±4.63g	4.19±0.21a
	0	0.036±0.001d	11.66±0.77e	70.33±5.13a	3.64±0.16b
	1	0.038±0.001cd	12.21±0.86de	66.19±4.37ab	3.48±0.14b
3	2	0.039±0.001bc	13.09±0.76d	61.57±4.57bc	3.03±0.21d
	3	0.040±.002abc	14.18±0.69c	53.33±5.36de	2. 68±0.19e
	4	0.042±0.002a	8.97±0.57f	43.47±3.59fg	4.47±0.11a

Values are given as mean±SD ($n=3$). Different lowercase superscript letters in the same column indicate significant differences ($p<0.05$)

distribution of ZnONP and aggregation of excess nanoparticles in protein matrix. An increase in incompatibility of the protein/ZnO composites with excess ZnONP content resulted in discontinuous film matrix. ZnO is hydrophobic and tends to aggregate when certain concentration is reached to reduce energy dissipated in the system (Zhou et al. 2009). The aggregate could impede the arrangement of protein domains and amorphous network of FPI/FSG film and consequently reduce the mechanical properties of films. Similarly, the decrease of the mechanical strength of whey protein isolate nanocomposite films was attributed to the non-uniform distribution of and aggregation of excess TiO_2 nanoparticles in film matrix (Zhou et al. 2009). The concentration of ZnONP was the major factor affecting structure and spatial organization of protein aggregates in film matrix. Thus, the incorporation of ZnONP at a particular level could manoeuvre the strength of resulting FPI/FSG films.

Water Vapour Permeability

WVP of FPI/FSG films prepared at pH 3 and pH 11 containing ZnONP at various levels are shown in Table 1. Myofibrillar proteins as the major component in FPI and alpha 1 and alpha 2 chains of gelatin are hydrophilic, due to its polar amino acids. Hydroxyl group (−OH) of glycerol used as a plasticiser also contribute to hydrophilicity of film. As a consequence, muscle protein and gelatin films had the lowered moisture barrier property (Prodpran et al. 2007).

WVP of FPI/FSG films decreased as the levels of ZnONP was increased up to 3 % ($p<0.05$), regardless of pH of FFS. However, FPI/FSG-ZnO nanocomposite films prepared at pH 11 with the same level of ZnONP had lower WVP than those prepared at pH 3 ($p<0.05$). This result was in agreement with the higher mechanical properties of the former, in which the stronger and more compact structure was formed. This effectively prevented the migration of water vapour through the films (Chen 1995). At a level of 3 %, ZnONP dispersed well in the matrix with few paths for water molecules to pass through. The significant decrease in WVP of film after the addition of ZnONP may be attributed to the greater water resistance of ZnONP. Thus, the incorporation of these nanoparticles to the protein matrix introduces a tortuous pathway for water vapour molecules to pass through (Alebooyeh et al. 2012; Yu et al. 2009). The improvement of water resistance in other nanocomposite systems containing ZnO fillers such as starch nanocomposites has also been reported (Alebooyeh et al. 2012).

When ZnONP at a level of 4 % was incorporated, the superfluous filler congregated easily, decreasing the effective content of the filler. Increased WVP of films containing 4 % ZnONP was associated with the poor mechanical properties of films caused by pronounced coagulation of proteins at high Zn^{2+} concentration. Arfat and Benjakul (2013) reported that disproportionate addition of Zn^{2+} causes protein coagulation in muscle proteins from yellow stripe trevally. Coagulated proteins along with the agglomerated ZnONP contributed to the poor integrity of the film matrix. As a consequence, increased WVP of films was obtained. Thus, both pH and ZnONP level had the profound impact on WVP of FPI/FSG films.

Colour Values

Table 2 shows the colour of FPI/FSG films prepared at pH 3 and pH 11 with varying levels of ZnONP. FPI/FSG films prepared at pH 11 had the lower L^*-value (lightness) and a^*-value (redness/greenness) but higher b^*-value (yellowness) and ΔE^* (total colour difference), compared with those prepared at pH 3, regardless of ZnONP content ($p<0.05$). This result suggested that an alkaline condition could induce the formation of yellowish pigment, especially via Maillard reaction. Alkaline pH favours the reductone formation over furfural production from the amadori products, leading to colour development in protein-based films (Tongnuanchan et al. 2011).

At both pH 3 and pH 11, the addition of ZnONP into the FPI/FSG film did not have a marked impact on L^*- and a^*-values ($p>0.05$). However, decreases in b^*- and ΔE^*-values were obtained as ZnONP with increasing amount was incorporated, regardless of the pH of FFS ($p<0.05$). These results were in agreement with Espitia et al. (2013) who reported that increasing amount of ZnONP markedly decreased b^*- and ΔE^*-values, whilst had no significant effect on L^*- and a^*-values of methyl cellulose (MC)-ZnO nanocomposite films. Such changes in colour of resulting films were most likely attributed to the whitening effect due to the presence of ZnONP (Espitia et al. 2013). The results suggested that ZnONP decreased yellowish colour in resulting nanocomposite films.

Light Transmittance and Transparency Values

Transmission of UV and visible light at wavelength range of 200–800 nm of FPI/FSG films prepared at different pH (3 or 11) and incorporated with ZnONP at different levels are shown in Table 2. Control films (without ZnONP) had a good barrier property in the UV-ranges (200–280 nm), irrespective of pH of FFS. Protein based films are generally known to have excellent UV barrier properties due to the presence of high content of aromatic amino acids which can absorb UV light (Hoque et al. 2011).

The percent transmittance (%T) of films in both UV and visible range decreased as the levels of ZnONP increased, regardless of pH of FFS. However, the %T of FPI/FSG-ZnO nanocomposite films prepared at pH 3 was higher than those of films prepared at pH 11. The results indicated that ZnONP were able to impede the light transmission through the film. This was mainly due to the hindrance of light passage or light

Table 2 Colour, light transmittance and transparency values of FPI/FSG-ZnONP films

pH level	ZnONP level (% *w*/*w*)	Colour parameters				Light transmittance (%)								Transparency value
		*L**	*a**	*b**	Δ*E**	200	280	350	400	500	600	700	800	
11	0	90.19±0.19d	−1.89±0.02b	3.84±0.17a	4.31±0.19a	0.00	6.72	54.73	60.17	71.22	72.68	79.49	82.15	3.95±0.03e
	1	90.24±0.23cd	−1.87±0.03b	3.45±0.14b	3.94±0.11b	0.00	1.68	49.5	50.58	65.2	70.12	76.07	78.78	4.04±0.03d
	2	90.29±0.13bcd	−1.88±0.02b	3.18±0.1c	3.76±0.13b	0.00	0.79	45.72	46.58	62.88	68.79	70.19	74.12	4.14±0.04c
	3	90.36±0.17abcd	−1.88±0.04b	2.91±0.09d	3.44±0.04c	0.00	0.33	41.57	40.98	58.91	67.22	68.77	72.43	4.22±0.05c
	4	90.40±0.20abcd	−1.85±0.04b	2.62±0.05e	3.09±0.09d	0.00	0.14	38.18	37.02	54.95	61.34	63.24	68.16	5.04±0.07a
3	0	90.52±0.17abc	−1.37±0.04a	2.26±0.06f	2.96±0.08d	0.00	7.30	68.44	72.19	75.17	77.27	86.42	87.11	3.18±0.02i
	1	90.57±0.15ab	−1.35±0.01a	2.03±0.04g	2.70±0.13e	0.00	1.84	61.66	63.26	70.2	75.01	80.59	83.37	3.29±0.05h
	2	90.6±0.10ab	−1.34±0.03a	1.79±0.06h	2.46±0.06f	0.00	0.86	50.14	54.04	66.18	73.5	77.32	80.94	3.42±0.04g
	3	90.62±0.13a	−1.35±0.02a	1.58±0.07i	2.32±0.09f	0.00	0.45	47.15	48.12	61.04	72.23	74.23	77.17	3.51±0.08f
	4	90.64±0.16a	−1.33±0.04a	1.36±0.06j	2.26±0.13f	0.00	0.21	43.3	44.56	57.88	65.15	70.04	73.83	4.44±0.07b

Values are given as mean±SD (n=3). Different lowercase superscript letters in the same column indicate significant differences (p<0.05)

scattering by the nanoparticles dispersed in the film matrix (Kanmani and Rhim 2014). The incorporation of ZnONP into the FPI/FSG films greatly reduced the transmission of UV light at 280 nm. Rouhi et al. (2013) reported that the gelatin films added with ZnO nanorods had lower transmission in the UV range. The FPI/FSG reinforced with ZnONP could be used as UV-shielding packaging films to prevent UV light, which can induce lipid oxidation of various foods. With increasing levels of ZnONP, the films also showed the lower transmittance in the visible ranges. ZnONP in film could act as the barrier towards light.

Control FPI/FSG films prepared at pH 3 showed lower transparency values than those prepared at pH 11, indicating that the former was more transparent. These results were in agreement with Tongnuanchan et al. (2011) who reported that films based on red tilapia (*Oreochromis niloticus*) muscle protein prepared at acidic condition (pH 3) were more transparent than those prepared at alkaline condition (pH 11). When FPI/FSG films were added with ZnONP, the higher transparency values were observed (p<0.05). The greater transparency value represents the lower transparency of film. For FPI/FSG-ZnO nanocomposite films, the transparency value increased as the level of ZnONP content increased (p<0.05), indicating the decrease in the transparency of resulting films. This was more likely due to the opaqueness of ZnONP, which was distributed throughout the films. Similarly, Kanmani and Rhim (2014) reported that the blending of silver nanoparticles with gelatin protein films reduced transparency of the films. Thus, both pH of FFS and the level of ZnONP had the impact on transparency and light barrier properties of FPI/FSG films.

Characteristics of FPI/FSG-ZnO Nanocomposite Films

The FPI/FSG films prepared at pH 3 and pH 11, containing ZnONP at 3 % level, which showed the improved mechanical and water vapour barrier properties, were characterised, in comparison with FPI/FSG films without ZnONP prepared at corresponding pH.

Wide Angle X-ray Diffraction Pattern

FPI/FSG films prepared at pH 3 and pH 11 without and with 3 % ZnONP were analysed using the WAXD technique in comparison with ZnONP (Fig. 1a, b). Pure ZnONP showed the main characteristic peaks at 2θ=31.7, 34.4, 36.2, 47.5, 56.6, 62.7 and 67.9, matching with the standard (JCPDS76-0704), confirming the hexagonal wurtzite structure of ZnONP (Bajpai et al. 2012). Films prepared at acidic and alkaline conditions showed almost similar pattern of WAXD. FPI/FSG film exhibited two broad diffraction peaks at 2θ around 9.72° and 21.87°, which represent its amorphous structure. Almost similar WAXD characteristic has been reported for films prepared from pig skin gelatin (Maria et al. 2008).

As shown in Fig. 1b, the control film prepared from FFS at both pHs did not reveal any sharp diffraction peak, whilst the FPI/FSG-ZnO nanocomposite film revealed distinctive diffraction peaks at 2θ=31.7, 34.4, 36.2, 47.5, 56.6, 62.7 and 67.9, corresponding to the (100), (002), (101), (102), (110), (103) and (200) planes of hexagonal wurtzite structure of ZnONP (Bajpai et al. 2012). These results confirmed that the hexagonal wurtzite structure of ZnONP was not affected after their incorporation in protein matrix. These typical WAXD peaks revealed the successful formation of FPI/FSG-ZnO nanocomposite.

FTIR Spectroscopy

FTIR spectra of FPI/FSG films prepared at pH 3 and pH 11 without and with 3 % ZnONP are shown in Fig. 1c. Films prepared at acidic and alkaline conditions showed similar

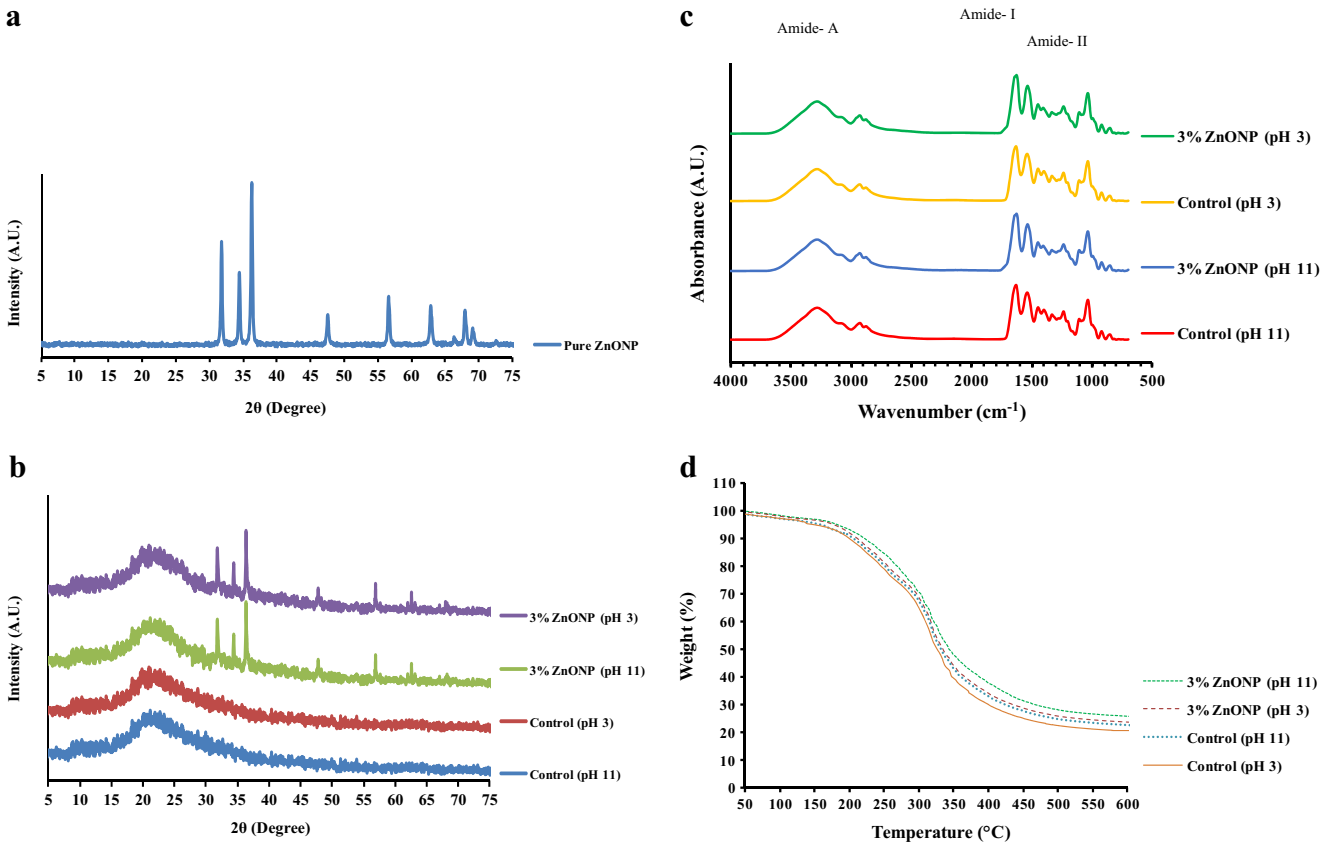

Fig. 1 WAXD patterns of pure ZnONP (**a**) and FPI/FSG films prepared at pH 3 and pH 11 without and with 3 % (*w*/*w*) ZnONP (**b**); ATR-FTIR spectra of FPI/FSG films prepared at pH 3 and pH 11 without and with 3 % (*w*/*w*) ZnONP (**c**) and TGA curves of FPI/FSG films prepared at pH 3 and pH 11 without and with 3 % (*w*/*w*) ZnONP (**d**)

major peaks but the amplitudes of peaks varied slightly. Generally, all films had the similar spectra in the range of 1800–600 cm^{-1}, covering amide-I, II and III bands. All films exhibited the major bands at around 1629–1632 cm^{-1} (amide-I, representing C=O stretching/hydrogen bonding coupled with COO), 1536 cm^{-1} (amide-II, arising from bending vibration of N–H groups and stretching vibrations of C–N groups) and 1238 cm^{-1} (amide-III, representing the vibrations in plane of C–N and N–H groups of bound amide or vibrations of CH_2 groups of glycine) (Muyonga et al. 2004). Yakimets et al. (2005) reported the similar result for bovine skin gelatin film, where amide-I, amide-II and amide-III peaks were found at the wavenumbers of 1633, 1536 and 1240 cm^{-1}, respectively. The band situated at the wavenumber of 1036–1039 cm^{-1} was found in all film samples, corresponding to the interactions arising between plasticiser (OH group of glycerol) and film structure (Hoque et al. 2011). An amide-A band was observed at the wavenumber of 3275–3280 cm^{-1} for all film samples. Amide-B band was also found at 2926–2928 cm^{-1} for all film samples. The amide-A band represents the NH-stretching coupled with hydrogen bonding, and amide-B band represents the asymmetric stretching vibration of CH as well as NH_3^+ (Hoque et al. 2011; Muyonga et al. 2004).

The slight shift of FTIR spectra of films with 3 % ZnONP in the amide-I region to the lower wavenumber were mainly associated with interaction of carbonyl of polypeptide chains with ZnONP. The shifts of the amide-I peak to a lower wavenumber were related to a decrease in the molecular order (Rouhi et al. 2013). Furthermore, for films prepared at pH 3, the amide-A band from the N–H stretching vibration of the hydrogen bonded N–H group became visible at wavenumbers 3280 and 3278 cm^{-1} for the control film and 3 % ZnONP incorporated film, respectively, and at 3278 and 3275 cm^{-1} for the control film and 3 % ZnONP incorporated film prepared at pH 11, respectively. This result clearly showed that amide-A band shifted to lower wavenumber when ZnONP was added. The shift to the lower wavenumber in the amide-A region suggested that N–H groups with protein chain interact with ZnONP, mainly via hydrogen bonding (Nikoo et al. 2011). Rouhi et al. (2013) reported similar results from gelatin-based nanocomposite films incorporated with ZnO nanorods. Therefore, FTIR results reconfirm the interaction between protein molecules and ZnONP which was responsible for the improved mechanical and water vapour barrier properties of resulting FPI/FSG nanocomposite films (Table 1).

Thermo-Gravimetric Analysis

TGA thermograms revealing thermal degradation behaviour of FPI/FSG films prepared at pH 3 and pH 11 without and with 3 % ZnONP are shown in Fig. 1d. Their corresponding thermal degradation temperatures (T_d) and weight loss (Δw) are presented in Table 3. Three main stages of Δw were observed for all films. The first stage weight loss (Δw_1=2.28–3.14 %) was observed over the temperature (T_{d1}) ranging from 47.22 to 51.27 °C up to approximately 150 °C, possibly associated with the loss of free and bound water adsorbed in the film. The similar result was found in cuttlefish skin gelatin film (Hoque et al. 2011) and porcine plasma protein film added with different cross-linking agents (Nuthong et al. 2009). The second stage weight loss (Δw_2=24.66–27.86 %) appeared at the onset temperature of 195.23−213.47 °C (T_{d2}), depending on the film samples. This was most likely due to the degradation or decomposition of lower molecular weight protein fractions and glycerol compounds. For the third stage of weight loss (Δw_3=42.64–45.61 %), T_{d3} of 299.1 −319.52 °C was observed for all films but varied with film samples. This was possibly due to the decomposition of highly interacted proteins in film matrix.

The results suggested that films with ZnONP showed enhanced thermal stability in comparison with the films without ZnONP. ZnONP in the FPI/FSG matrix could insert within film matrix or act as thermal insulator or mass transport barrier to volatile products generated during decomposition. This resulted in delay of thermal degradation and improved thermal stability of the composites. The increase in the thermal stability was in agreement with the increase in mechanical resistance due to the strong film network, more energy thus being required to decompose the films. Carboxymethyl cellulose/ZnO nanocomposite film with a high concentration of ZnONP showed enhanced thermal stability in comparison with control film (Espitia et al. 2013). Nevertheless, films prepared at pH 11 showed higher heat stability than those prepared at pH 3, irrespective of ZnONP addition. Amongst all films, films prepared at pH 11 and containing 3 % ZnONP had the highest thermal degradation/decomposition temperature (T_{d2}=213.47 and T_{d3}=319.52). Higher amount of disulphide and hydrophobic interaction between proteins in FPI at alkaline conditions might contribute to heat resistance of their films (Tongnuanchan et al. 2011). Moreover, at alkaline pH, the salt bridge interactions between ZnO and proteins mostly yielded the stronger film network, leading to higher heat resistance of the resulting nanocomposite films than control films.

Additionally, all films had residual mass (representing char content) at 600 °C in the range of 23.39 %–30.42 %. The highest char content observed in nanocomposite film prepared at pH 11 containing 3 % ZnONP was most likely ascribed to the high thermal stability of the ZnONP and the highest bonding formed in the protein network. Thus, both pH and incorporated ZnONP, affected thermal property of FPI/FSG films.

Scanning Electron Microscopy Visualisation

SEM micrographs of the surface and freeze-fractured cross-section of FPI/FSG films prepared at pH 3 and pH 11 without and with 3 % ZnONP are illustrated in Fig. 2. At both pHs 3 and 11, the slightly rough surface was noticeable in the control FPI/FSG film (without ZnONP). Arrangements or alignments of FPI and FSG might not occur in an ordered fashion. From SEM images, no distinct separation was observed in the matrix of FPI/FSG film. Roughness of surface structure was more pronounced in films incorporated with ZnONP than that found in the control film, regardless of pH of FFS. The roughness of film was attributed to ZnONP distributed throughout the film matrix. This might be also associated with the coexisting protruded film structure as indicated by the increased thickness of resulting films (Table 1). Furthermore, nanocomposite films showed distinctive ZnONP images on their film surfaces, in which ZnONP was uniformly dispersed in the films.

The discontinuous zone or microcracks were found in FPI/FSG film prepared at pHs 3 and 11. This was more likely related with less interaction between molecules of FPI and FSG. This could be associated with poorer TS and WVP of FPI/FSG films. However, crack-free cross-sectional structure with distinctive ZnONP images was observed in FPI/FSG films incorporated with 3 % ZnONP (at both pHs), compared

Table 3 Thermal degradation temperature (T_d, °C) and weight loss (Δw, %) of FPI/FSG films containing 0 and 3 % ZnONP

pH level	ZnONP level (% *w*/*w*)	Δ_1		Δ_2		Δ_3		Residue (%)
		T_{d1},onset	Δw_1	T_{d2},onset	Δw_2	T_{d3},onset	Δw_3	
11	0	49.17	2.55	201.04	26.08	303.22	44.86	26.51
11	3	51.27	2.28	213.47	24.66	319.52	42.64	30.42
3	0	47.22	3.14	195.23	27.86	299.1	45.61	23.39
3	3	49.82	2.87	200.37	25.79	306.01	43.43	27.91

Δ_1, Δ_2 and Δ_3 denote the first, second and third stage weight loss, respectively, of film during heating scan

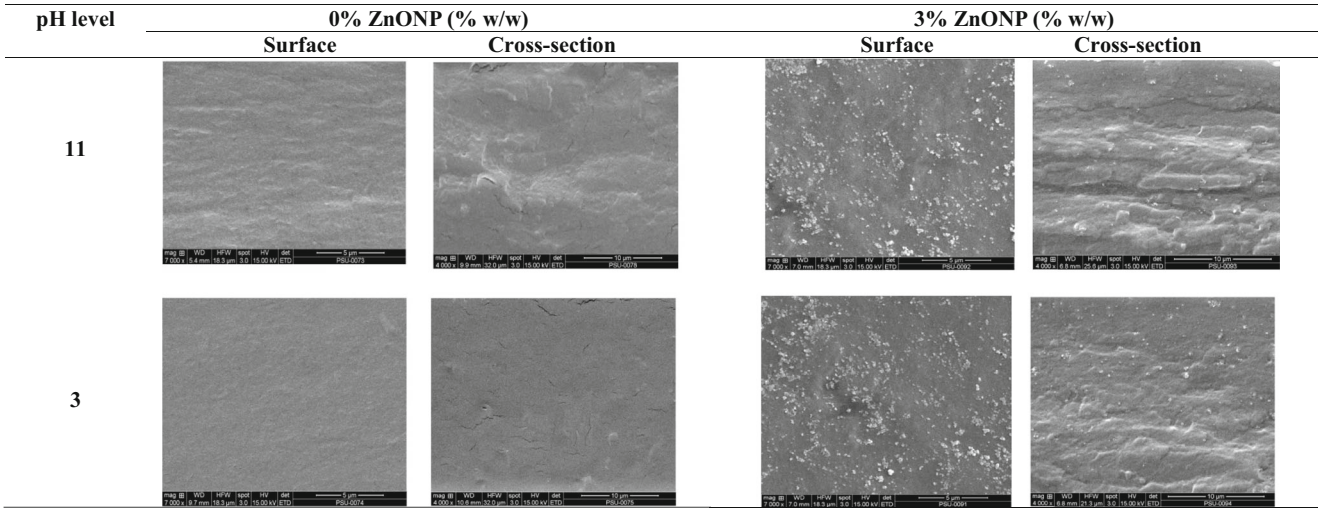

Fig. 2 SEM micrographs of surface and freeze-fractured cross-section of FPI/FSG films prepared at pH 3 and pH 11 without and with 3 % (*w*/*w*) ZnONP. Magnification ×7000 and ×4000 for surface and cross-section, respectively

with those observed in FPI/FSG blend film. This was plausibly due to the filler property of ZnONP and its interaction with FPI/FSG protein molecules in the film matrix. The ZnONP could impede the water molecules to transfer or penetrate through the film (Alebooyeh et al. 2012). As a result, the WVP of ZnONP incorporated films was lowered, compared with the control film, as shown in Table 1. Thus, the microstructures of films were markedly governed by ZnONP incorporation.

Antimicrobial Activity of FPI/FSG-ZnO Nanocomposite Films

The antibacterial activity of the FPI/FSG-ZnO nanocomposite films prepared at pH 3 and pH 11 with different ZnONP contents was tested using Gram-positive food pathogenic bacteria (*L. monocytogenes*) and Gram-negative food spoilage bacteria (*P. aeruginosa*) in comparison with the control FPI/FSG films, as shown in Fig. 3. At both pHs 3 and 11, the inhibition zone of ZnO-incorporated films increased with increasing ZnONP contents ($p<0.05$). At the same ZnONP content, antibacterial activity of FPI/FSG-ZnO nanocomposite films prepared at pH 3 was higher than those prepared at pH 11 ($p<0.05$). This was more likely governed by higher solubility of the films prepared at pH 3. Higher solubility of films prepared at pH 3 was obtained than those prepared at pH 11 (data not shown). ZnONP could be co-released with solubilised film matrix to a higher extent. The antimicrobial component releasing rate of gelatin films increased with increasing solubility (Yehuala and Emire 2013).

The strong antimicrobial activity of ZnONP and the mechanism of the action against the microorganisms have been demonstrated (Espitia et al. 2013; Zhang et al. 2010). The release of Zn^{2+} ions from the powder could penetrate through the cell wall of microorganism and react with interior components that finally affect the viability of the cells. ZnO has also been known to mediate the generation of hydrogenperoxide (H_2O_2), a powerful oxidizing agent causing damage to the cell membrane of bacteria (Tayel et al. 2011).

At the same ZnONP level, the antibacterial effect of the FPI/FSG-ZnO nanocomposite films on *L. monocytogenes*

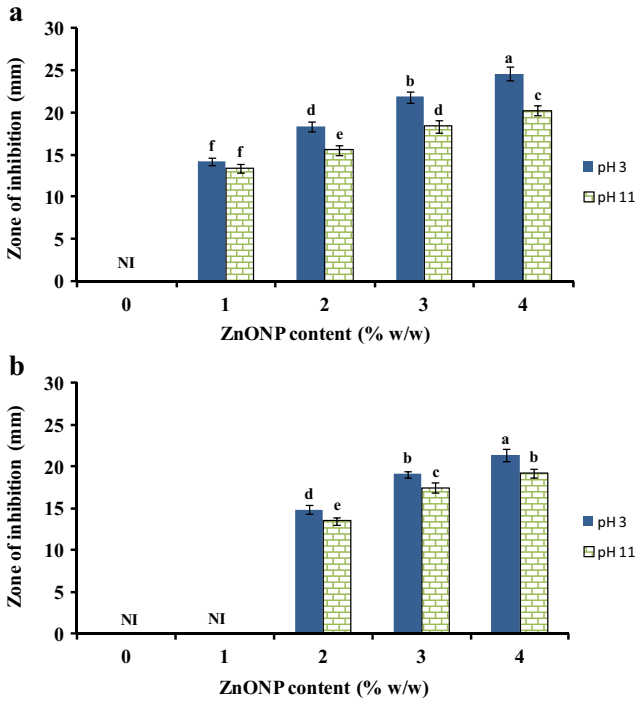

Fig 3 Effects of ZnONP content on antimicrobial activity of FPI/FSG films prepared at pH 3 and pH 11 against *L. monocytogenes* (**a**) and *P. aeruginosa* (**b**). *Bars* represent the standard deviation ($n=3$). Different lowercase letters on the bars indicate significant differences ($p<0.05$). NI indicates the absence of inhibitory zone

was stronger than on *P. aeruginosa*, regardless of pH of FFS. Tam et al. (2008) demonstrated that ZnO was more effective in killing Gram-positive than Gram-negative bacteria. Gram-positive bacteria typically have one cytoplasmic membrane and cell wall composed of peptidoglycan (Ma and Zhang 2009). The more complex cell wall structure of the Gram-negative bacteria, with a layer of peptidoglycan between the outer membrane and the cytoplasmic membrane might prevent ZnONP penetration into the cells and interaction with their internal components (Ma and Zhang 2009). Antibacterial action of ZnONP is suggested to occur through its interaction with specific cell compounds like surface proteins (e.g. adhesions) and teichoic acids plus lipoids (forming lipoteichoic acids), which may be found in Gram-positive rather than in Gram-negative bacteria (Tayel et al. 2011). However, further studies are required to clarify the exact antibacterial mechanism of ZnONP. Thus, FPI/FSG nanocomposite films, especially those prepared at pH 3, had the potential to control both *L. monocytogenes* and *P. aeruginosa* in foods.

Conclusion

The antimicrobial nanocomposite films based on FPI/FSG were developed by addition of ZnONP. Properties of FPI/FSG films could be enhanced by incorporating 3 % ZnONP at both acidic and alkaline pH. Nanocomposite film showed the improved mechanical, water vapour barrier and thermal properties, compared with control films (without ZnONP). Incorporation of ZnONP yielded film with lower yellow discoloration. Moreover, FPI/FSG-ZnO nanocomposite films inhibited the growth of Gram-positive (*L. monocytogenes*) and Gram-negative food borne pathogenic and spoilage bacteria (*P. aeruginosa*). Thus, FPI/FSG-ZnO nanocomposite films could be used as an active food packaging to prevent growth of pathogen and spoilage bacteria in foods.

Acknowledgments The authors would like to express their sincere thanks to Prince of Songkla University and National Research Council of Thailand for their financial support. The TRF Senior Research Scholar programme is gratefully acknowledged.

References

Alebooyeh, R., Nafchi, A. M., & Jokar, M. (2012). The effects of ZnO nanorods on the characteristics of sago starch biodegradable films. *Journal of Chemical Health Risks, 2*, 13–16.

AOAC. (2000). *Official methods of analysis*. Washington, DC: Association of Official Analysis Chemists.

Arfat, Y. A., & Benjakul, S. (2013). Gel strengthening effect of zinc salts in surimi from yellow stripe trevally. *Food Bioscience, 3*, 1–9.

Arfat, Y. A., Benjakul, S., Prodpran, T., & Osako, K. (2014). Development and characterisation of blend films based on fish protein isolate and fish skin gelatin. *Food Hydrocolloids, 39*, 58–67.

Bajpai, K. S., Chand, N., & Chaurasia, V. (2012). Nano zinc oxide-loaded calcium alginate films with potential antibacterial properties. *Food and Bioprocess Technology, 5*, 1871–1881.

Chen, H. (1995). Functional properties and applications of edible films made of milk proteins. *Journal of Dairy Science, 78*, 2563–2583.

Chinabhark, K., Benjakul, S., & Prodpran, T. (2007). Effect of pH on the properties of protein-based film from bigeye snapper (*Priacanthus tayenus*) surimi. *Bioresource Technology, 98*, 221–225.

Clinical and laboratory standards institute (2007). *Performance standards for antimicrobial susceptibility testing*; *Seventeenth information supplement*. CLSI document M100-S17 ISBN 1-56238-625-5). Clinical and Laboratory Standards Institute, 940 West Valley Road, Suite 1400, Wayne, Pennsylvania 19087–1898 USA.

Clinical and laboratory standards institute (2010). *Methods for antimicrobial dilution and disk susceptibility testing of infrequently isolated or fastidious bacteria*; *Approved guideline—second edition*. CLSI document M45-A2 ISBN 1-56238-732-4). Clinical and Laboratory Standards Institute, 940 West Valley Road, Suite 1400, Wayne, Pennsylvania 19087–1898 USA.

Espitia, P. J. P., et al. (2013). Physical–mechanical and antimicrobial properties of nanocomposite films with pediocin and ZnO nanoparticles. *Carbohydrate Polymers, 94*, 199–208.

Gennadios, A., Weller, C. L., Hanna, M. A., & Froning, G. W. (1996). Mechanical and barrier properties of egg albumin films. *Journal of Food Science, 61*, 585–589.

Han, J. H. (2000). Antimicrobial food packaging. *Food Technology, 54*, 56–65.

Han, J. H., & Floros, J. D. (1997). Casting antimicrobial packaging films and measuring their physical properties and antimicrobial activity. *Journal of Plastic Film and Sheeting, 13*, 287–298.

Hoque, M. S., Benjakul, S., Prodpran, T., & Songtipya, P. (2011). Properties of blend film based on cuttlefish (*Sepia pharaonis*) skin gelatin and mungbean protein isolate. *International Journal of Biological Macromolecules, 49*, 663–673.

Iwata, K., Ishizaki, S., Handa, A., & Tanaka, M. (2000). Preparation and characterization of edible films from fish water-soluble proteins. *Fisheries Science, 66*, 372–378.

Jongjareonrak, A., Rawdkuen, S., Chaijan, M., Benjakul, S., Osako, K., & Tanaka, M. (2010). Chemical compositions and characterization of skin gelatin from farmed giant catfish (*Pangasianodon gigas*). *LWT-Food Science and Technology, 43*, 161–165.

Kanmani, P., & Rhim, J. W. (2014). Physical, mechanical and antimicrobial properties of gelatin based active nanocomposite films containing AgNPs and nanoclay. *Food Hydrocolloids, 35*, 644–652.

Kovacevic, V., Vrsaljko, D., Lucic'Blagojevic, S., & Leskovac, M. (2008). Adhesion parameters at the interface in nanoparticulate filled polymer systems. *Polymer Engineering & Science, 48*, 1994–2002.

Ma, X. Y., & Zhang, W. D. (2009). Effects of flower-like ZnO nanowhiskers on the mechanical, thermal and antibacterial properties of waterborne polyurethane. *Polymer Degradation and Stability, 94*, 1103–1109.

Maria, T. M. C., Carvalho, R. A., Sobral, P. J. A., Habitante, A. M. B. Q., & Solorza-Feria, J. (2008). The effect of the degree of hydrolysis of the PVA and the plasticizer concentration on the color, opacity, and thermal and mechanical properties of films based on PVA and gelatin blends. *Journal of Food Engineering, 87*, 191–199.

McHugh, T. H., Aujard, J. F., & Krochta, J. M. (1994). Plasticized whey protein edible films: water vapor permeability properties. *Journal of Food Science, 59*, 416–423.

Muyonga, J. H., Cole, C. G. B., & Duodu, K. G. (2004). Characterisation of acid soluble collagen from skins of young and adult Nile perch (*Lates niloticus*). *Food Chemistry, 85*, 81–89.

Nikoo, M., Xu, X., Benjakul, S., Xu, G., Ramirez-Suarez, J. C., Ehsani, A., Kasankala, L. M., Duan, X., & Abbas, S. (2011). Characterization of gelatin from the skin of farmed Amur sturgeon (*Acipenser schrenckii*). *International Aquatic Research, 3*, 135–145.

Nuthong, P., Benjakul, S., & Prodpran, T. (2009). Characterization of porcine plasma protein-based films as affected by pretreatment and cross-linking agents. *International Journal of Biological Macromolecules, 44*, 143–148.

Prodpran, T., Benjakul, S., & Artharn, A. (2007). Properties and microstructure of protein-based film from round scad (*Decapterus maruadsi*) muscle as affected by palm oil and chitosan incorporation. *International Journal of Biological Macromolecules, 41*, 605–614.

Rouhi, J., Mahmud, S., Naderi, N., Ooi, C. H. R., & Mahmood, M. R. (2013). Physical properties of fish gelatin-based bio-nanocomposite films incorporated with ZnO nanorods. *Nanoscale Research Letters, 8*, 364–370.

Shi, L., Zhou, J., & Gunasekaran, S. (2008). Low temperature fabrication of ZnO-whey protein isolate nanocomposite. *Materials Letters, 62*, 4383–4285.

Shiku, Y., Hamaguchi, P. Y., Benjakul, S., Visessanguan, W., & Tanaka, M. (2004). Effect of surimi quality on properties of edible films based on Alaska pollack. *Food Chemistry, 86*, 493–499.

Sothornvit, R., Rhim, J.-W., & Hong, S.-I. (2009). Effect of nano-clay type on the physical and antimicrobial properties of whey protein isolate/clay composite films. *Journal of Food Engineering, 91*, 468–473.

Steel, R. G. D., & Torrie, J. H. (1980). *Principle and procedure of statistics* (2nd ed.). New York: McGraw-Hill.

Tam, K. H., Djurisic, A. B., Chan, C. M. N., Xi, Y. Y., Tse, C. W., Leung, Y. H., Chan, W. K., Leung, F. C. C., & Au, D. W. T. (2008). Antibacterial activity of ZnO nanorods prepared by a hydrothermal method. *Thin Solid Films, 516*, 6167–6174.

Tayel, A. A., El-Tras, W. F., Moussa, S., El-Baz, A. F., Mahrous, H., Salem, M. F., & Brimer, L. (2011). Antibacterial action of zinc oxide nanoparticles against foodborne pathogens. *Journal of Food Safety, 31*, 211–218.

Tongnuanchan, P., Benjakul, S., Prodpran, T., & Songtipya, P. (2011). Characteristics of film based on protein isolate from red tilapia muscle with negligible yellow discoloration. *International Journal of Biological Macromolecules, 48*, 758–767.

Yakimets, I., Wellner, N., Smith, A. C., Wilson, R. H., Farhat, I., & Mitchell, J. (2005). Mechanical properties with respect to water content of gelatin films in glassy state. *Polymer, 46*, 12577–12585.

Yehuala, G. A., & Emire, S. A. (2013). Antimicrobial activity, physicochemical and mechanical properties of Aloe (*Aloe debrana*) based packaging films. *British Journal of Applied Science & Technology, 3*, 1257–1275.

Yu, J., Yang, J., Liu, B., & Ma, X. (2009). Preparation and characterization of glycerol plasticized-pea starch/ZnO-carboxymethylcellulose sodium nanocomposites. *Bioresource Technology, 100*, 2832–2841.

Zhang, L., Jiang, Y., Ding, Y., Daskalakis, N., Jeuken, L., Povey, M., O'Neill, A., & York, D. (2010). Mechanistic investigation into antibacterial behaviour of suspensions of ZnO nanoparticles against *E. coli*. *Journal of Nanoparticle Research, 12*, 1625–1636.

Zhou, J. J., Wang, S. Y., & Gunasekaran, S. (2009). Preparation and characterization of whey protein film incorporated with TiO_2 nanoparticles. *Journal of Food Science, 74*, N50–N56.